Final Technical Report
Research Grant NGR 33-010-145

submitted to the

National Aeronautics and Space Administration

by

Laboratory of Nuclear Studies
Cornell University
Ithaca, New York 14853

Title: Cosmic Gamma-Ray Telescope

Principal Investigator: Kenneth Greisen
Professor of Physics
S.S. No. [redacted]
Telephone 607-256-3427

Period Covered by Proposal:

November 1, 1970 - February 28, 1976

Date of this Report: June 1976

Kenneth Greisen
Principal Investigator

NASA Technical Officer - Albert G. Opp

(NASA-CR-148681) COSMIC GAMMA-RAY TELESCOPE Final Technical Report, 1 Nov. 1970 - 28 Feb. 1976 (Cornell Univ., Ithaca, N.Y.) 22 p

N76-77702

Unclas
00/98 50394

TABLE OF CONTENTS

I. Objectives of the Research

High-energy gamma radiation is one of the many means of probing the universe. It originates both at intense discrete objects, such as pulsars, and in interstellar space. Its dominant processes of origin are different from those of x-rays, of radio waves, and of infra-red, ultra-violet or visible light; and hence it reveals different features of the sources, including the presence of high-energy nuclei and electrons, and the nature of the ambient medium (gas, magnetic field or low-energy radiation field) with which these particles interact.

The total energy in the gamma-ray part of the eletromagnetic spectrum is not especially small, but the average number of gamma rays per unit of area and time is very low. To combat this limitation, detectors of large size are needed. Because other forms of radiation (particularly cosmic-ray particles) are much more numerous than the gamma rays, the detector must have excellent selectivity. Good angular resolution is vital. And to avoid both absorption of the cosmic gamma rays in the atmosphere and flooding them with a background of secondary gamma rays, the instruments must be deployed above as much of the atmosphere as possible.

With these needs in mind, the Cornell group set out to develop a high-energy gamma-ray telescope based on the Cerenkov radiation emitted in a low density gas by electron-positron pairs produced by the gamma rays in a thin converter. This method passively rejects cosmic-ray background with high efficiency, and permits utilization of a very large collecting area (5 square meters in this instance) without complicating the recording system. It is

sensitive to gamma rays above 150 MeV, provides rough but improvable energy resolution up to at least 1000 MeV, and good angular resolution (0.5 degrees for gammas above 1000 MeV). A prototype instrument was to be designed that would be suitable for balloon flights with radio-controlled pointing of the telescope, and point sources of high-energy gamma rays were to be studied with this instrument. Balloon flights suffer from too much atmospheric background to permit good studies of the diffuse component of celestial gamma radiation, and drastically degrade the sensitivity to point sources as well (because of brevity of exposure times as well as the background). However, experience with the balloon-borne instrument was regarded as an initial step in providing specifications for a future telescope in space.

II. Chronological Summary of Research Activity

Prior to the period of this grant, initial steps in the design of the gas Cerenkov telescope were carried out at Cornell with support from the AFOSR. Temporary collaboration was arranged with the Smithsonian Astrophysical Observatory (G.G. Fazio, D.R. Hearn, and H.F. Helmken), who designed the orientation system. Beginning in November, 1970, after support from the AFOSR was withdrawn for lack of military relevancy, NASA provided grants which permitted completion of the instrument development and the carrying out of balloon flights.

Altogether, six flights have been conducted, all from the National Scientific Balloon Facility at Palestine, Texas. These flights may be summarized as follows:

#1	February 13, 1971	Results limited by freezing of the azimuth control system at ceiling altitude
#2	October 6, 1971	Directed at the Crab Nebula; discovered gamma rays up to more than 1000 MeV emitted by the pulsar NP0532.
#3	February 18, 1972	Balloon failure during ascent
#4	September 9, 1972	Directed at sources in the Cygnus region; only upper limits of flux established.
#5	July 23, 1973	Directed at the Crab Nebula; discovered drastic reduction in highest-energy gammas from NP0532.
#6	July 22, 1974	Directed at the Crab Nebula; found gamma-ray flux from NP0532 had returned to 1971 value.

III. Description of the High-Energy Telescope

A schematic diagram of the instrument is shown in Figure 1 and a picture of the internal assembly is given in Figure 2. For balloon flights, the structure shown in the photograph is enclosed in a neoprene-lined fiberglas bag. This is filled with a freon-air mixture at sea level. The gas is vented during balloon ascent until a pressure of 1.6 psi is reached, at which time the valve is closed to maintain the desired gas density and index of refraction.

Principles of Gamma-Ray Recognition

Charged particles entering the front end of the detector are vetoed by producing signals in the first scintillator. A gamma ray

produces no response in this scintillator, but may convert (with 20% efficiency) to an electron-positron pair in the thin lead sheet (1.6mm thick) directly under it. These charged particles produce a signal in the scintillator immediately under the lead, and another signal, 17 ns later, in a scintillator beyond the mirror at the exit end of the instrument. While traversing the gas, the electron and positron emit narrow cones of Cerenkov light, which are focussed by the telescope mirror onto a set of seven phototubes (each 20 cm diameter) in the focal plane, arriving 32 ns after the intital signal. A gamma ray parallel to the axis is recognized by producing an optical signal in the central phototube, properly delayed with respect to the sequential signals in the second and third scintillators, and unaccompanied by a veto pulse in the first scintillator. Gamma rays in directions slightly off axis are similarly recognized, except that the Cerenkov light is displaced from the center of the focal plane; the off-set angle of the gamma ray is determined from the position of the centroid of the pool of light in this place.

The low gas density sets an energy threshold. In a gas of index of refraction η, Cerenkov light is only produced by charged particles with velocity $v>c/\eta$, and thus with energy exceeding $mc^2(\eta/\sqrt{\eta^2}-1) \simeq mc^2/\sqrt{2(\eta-1)}$. In our low density gas, $\eta-1 \simeq 7\times10^{-5}$ and the threshold energy is about 80 mc^2. This reinforces the cosmic-ray particle rejection by the veto scintillator, since less than one percent of the charged cosmic-ray particles have enough energy to produce Cerenkov radiation in the gas. For electrons

and positrons, however, the threshold energy (about 40 MeV) is much lower than for nuclei and mesons. Thus gamma rays can produce detectable signals if their energy exceeds about 100 MeV.

Exposure Factor

The mean sensitive diameter of the scintillators is 2.5 meters and the collecting area is 4.6 m^2. The gamma-ray conversion efficiency is 0.20. Thus the effective collecting area is 9200 cm^2. At balloon altitudes, absorption of the primary gamma rays in the overlying air generally degrades this effective area to about 8000 cm^2.

A balloon flight directed at a point source can usually achieve several hours with the source in view at a high zenith angle. Thus, the exposure factor for a point source is about 10^8 cm^2-s, so that sources with strength between 10^{-7} and 10^{-6} photons /cm^2-s can produce to 10 to 100 recorded events in a single flight.

The angular field of view is limited primarily by the size of the phototube array in the focal plane and the focal length of the mirror. In our case the angular diameter was about 7 degrees and the solid angle .012 sr, making the effective area times solid angle about 100 cm^2-sr and the trigger rate at a pressure of 5 g/cm^2 about 0.8 per second. (Outside the atmosphere, this rate would only be about 10 per hour, greatly improving the detectability of faint sources.)

Background and Sensitivity

The rejection of events initiated by charged particles and by gamma rays outside the telescope aperture has been found to be practically perfect. Indeed, the entire trigger rate at balloon altitudes is well accounted for by the atmospheric gamma rays. This is in great contrast to the general experience with spark chambers, where only a small fraction of the triggering events can usually be attributed to gamma rays. The reasons for this difference are several: the excellant geometry of the telescope's triggering and veto scintillators, the drastic elimination of charged particle triggers by the gas-Cerenkov system, the sharp angular collimation imposed by this system, and the strict requirements imposed on the time sequence of pulses contributing to the event signatures.

At balloon altitudes (say 5 g/cm^2) the background is due to atmospheric gammas and is about $5 \times 10^{-3} cm^{-2} s^{-1} sr^{-1}$ above the instrument's effective threshold of 160 MeV. For all events above threshold, assuming a dE/E^2 spectrum, the angular resolution is about 2^o, or 4×10^{-3}sr. In a flight with exposure factor $10^8 cm^2 sec$, the number of background events in 4×10^{-3} sr is about 2000. If the field of view under examination contains a point source, this will be detectable if the number of source events is large compared with the standard deviation in the background, $\sqrt{2000} \simeq 50$. Thus the minimum detectable source must yield at least 200 events, or have a flux of about 2×10^{-6} photons $cm^{-2} s^{-1}$.

With this instrument, as explained below, it is also possible to define a higher energy threshold, up to about 1000 MeV, and achieve an angular resolution of 0.5^{o}, or 2.5×10^{-4}sr. With the same exposure factor as above, the number of background events in this solid angle is then only 100, with a standard deviation of 10. At this energy, therefore, a source that yields only 40 events, and hence has a flux of about $4 \times 10^{-7} cm^{-2} s^{-1}$, would be detectable.

Pulsed sources are more easily detected because the relevant background is only that which occurs during the pulse on-time. Since this is typically 10% of the total time, the detectable average flux is lower than for a steady source by a factor of about 3.

In a space environment, the background is lower than that assumed above by a factor of 100 to 1000 depending on the pointing direction. The exposure time to a point source can easily be 10^{6}sec (intermediate between the values used by SAS-2 and COS-B) instead of 10^{4}sec as assumed for a balloon flight. Since the detectable flux varies as the square root of the background flux and inversely as the square root of the observation time, sources at least 100 times weaker can be detected in space than from a balloon flight. Other vital advantages of the space environment area (a) the possible continuity of source observations, permitting delineation of changes in emission, and (b) the possible measurement of the diffuse gamma ray flux as well as that from point sources.

Angular and Energy Resolution

The chief contributer to imperfect angular resolution is the coulomb scattering of the positron and electron in the lead converter. The mean scattering angles are inversely proportional to the particle energies. For single events the errors are unpredictable, but for an assumed spectrum of gamma rays, one can calculate the distribution of errors. The errors are reduced by using the centroid of the light pools of the electron and positron to assign directions to the gamma rays. Numerical calculations for a dE/E^2 spectrum have shown that for all events above our effective threshold of 160 MeV, the average error is about 1.6^o, while for all events above 1000 MeV, the average error is about 0.4^o. These errors include the effects of the size of the photo-tubes in limiting the precision of location of the centroid of the light pools, but do not include errors in sensing the pointing direction of the telescope. However, it has been possible to keep the latter errors under 0.25^o.

Two effects make the Cerenkov pulse heights sensitive to the gamma-ray energy. One is the variation of the light emission as $1-(E_o/E)^2$ where E_o is the threshold energy and E the energy of the electron or positron. The other is the coulomb scattering, which separates the light pools of the electron and positron and frequently makes one of the pools miss, or partially miss, the phototube. Thus, one can raise the effective energy threshold by requiring larger pulses. For point sources, one can also raise the effective thres-hold by reducing the allowed angle between the source and the

apparent gamma-ray direction. Quantitative evaluation of the effects of these measures have been carried out by Monte Carlo procedures. In general, these provide the telescope with rough energy resolution between about 200 and 1000 MeV.

IV. Summary of Observations

A. The Crab Nebula Pulsar, NP0532

This pulsar was first detected with the Cornell telescope on flight 2, October 6, 1971. The undeniable evidence appeared in the phase histogram, sharing counts vs. time folded module the period of the Crab pulsar. This histogram showed peaks at precisely the times of both the primary pulse and interpulse as given by radio and optical observations (taking into account the changing position of the balloon, the variation of pulsar period with time, and the signal transmission times). When the events were sorted according to energy, the best signal to noise ratio was found for the highest-energy gamma rays, namely those above about 750 MeV (median energy about 1400 MeV). However, an independent lower-energy group (240-750 MeV) also showed significant peaks at the same times in the histogram. The probability that the combined set of peaks could be due to chance was less than one in a million. Moreover, when the rate (per unit solid angle) of events occurring in the pulse on-times was plotted vs. apparent angle of the gamma rays with respect to the Crab Nebula, a sharp maxium was seen at $\Theta=0$, falling sharply with a half-width of slightly less than one degree, as expected from the angular resolution of the telescope. Thus, there was no doubt that the

recorded events were due to the Crab pulsar.

By using the angular distribution of the events alone, ignoring the phase histograms, it was possible to get the total flux from the nebula at these energies. These results were less accurate than those for the pulsed flux, but indicated a total flux about double the pulsed flux: in other words, that the nebula was emitting about as many high-energy gamma rays as the pulsar.

The integral flux values for the Crab pulsar found on this flight, and shown on the graph in Figure 3, were:

$$I\ (>240\ \text{Mev}) = (14.5 \pm 4.5)\ 10^{-7}\ \text{photons/cm}^2\text{-s}$$
$$I\ (>750\ \text{MeV}) = (5.0 \pm 1.3)\ 10^{-7}\ \text{photons/cm}^2\text{-s}$$

The Crab pulsar was next observed on flight 5. This flight was technically superior to flight 2 in several respects: the altitude was higher, the exposure time was longer, and electronic improvements had increased the efficiency. Therefore it was expected that the signal from the Crab would be much stronger and clearer than on flight 2. Instead, however, the signal was barely observable. The integral flux above 240 MeV was only down by a factor of two, but the flux above the higher energy, which had formerly had the greatest statistical significance, was now down by an apparent factor of seven, and could even have been zero. A thorough study ascertained that this loss of signal was not due to experimental or analytical error. This was further verified

by positive results of an x-ray detector carried on the same balloon flight for NRL (J. Kurfess and R. Bleach) and pointed parallel to the gamma-ray telescope: the pulsed x-ray flux was normal in intensity, and the period and phase agreed with the values assumed in our analysis.

Therefore, flight 5 led to the conclusion that drastic change can occur in the intensity of the pulsed radiation at very high energy. This had been unexpected, because in the optical and x-ray ranges, many observations of NP0532 had shown this pulsar to be very constant. Major variations have been observed in the radio pulse amplitudes, but these changes can be due to scattering effects not present at high frequency. However, there are physical processes with very high energy threshold (such as pair creation by photons in a strong magnetic field), that could account for extinction of high-energy gammas without affecting the x-ray, optical or lower-frequency radiation.

The time-averaged pulsed flux values determined for flight 5 (July 23, 1973) were

$$I\ (>240\ \text{MeV}) = (7.3 \pm 2.3)\ 10^{-7}\ \text{photons/cm}^2\text{-s}$$
$$I\ (>750\ \text{MeV}) = (0.68 \pm 0.53)\ 10^{-7}\ \text{photons/cm}^2\text{-s}$$

No steady flux from the nebular was discernible on this flight. However, the observation of a DC flux on the earlier flight was not sufficiently certain to permit a conclusion that the nebular flux, as well as the pulsed flux, had undergone a reduction.

At much higher energies, near 10^{12} eV, J. Grindlay and G. Fazio et al (Smithsonian Astrophysical Observatory) have reported apparent gamma radiation from the Crab that is variable in both phases of the pulsed flux and intensity. Since this radiation, if real, is not emitted in phase with the 10^{9} eV and lower energy components, the source region and processes of emission and absorption of the 10^{12} eV radiation may not have a close connection with our observations.

A third observation of the Crab pulsar was carried out on balloon flight 6, July 22, 1974. On this flight an electronic failure prevented establishing the same energy thresholds as on the two previous flights. However, the following integral flux values were deduced:

$$I\ (>200\ \text{MeV}) = (9.3 \pm 5.6)\ 10^{-7}\ \text{photons/cm}^2\text{-s}$$
$$I\ (>450\ \text{MeV}) = (7.0 \pm 2.3)\ 10^{-7}\ \text{photons/cm}^2\text{-s}$$

These agree quite well with the values obtained on flight 2, indicating a recovery from the "low state" that existed on July 23, 1973.

The intensities observed on all three flights are shown in Figure 3 along with spectral points obtained by the SAS-2 satellite (D. Kniffen et al, Nature 251, 397 (1974)). These are the best data available for comparison with our own; and recent reports of observations by COS-B (the Caravane Collaboration of ESA, reporting at the 1976 Goddard Gamma-Ray Conference) indicate close agreement

with SAS-2. Considering the difference in the instruments and possible errors in their calibrations, one must admit that all the points in Figure 3 are in substantial agreement except for the high-energy point of our flight 5, when for a still undetermined reason, the Crab pulsar turned off its radiation above about 400 MeV. (The dashed line in Figure 3 connects with x-ray data in the energy range 10-300 keV.)

B. Other Sources

On flight 4 (September 9, 1972), the telescope was pointed for brief periods at balloon altitude towards six different sources in the Cygnus region. A communication malfunction during the ascent of the balloon resulted in venting more gas than was desired, reducing the pressure to 1/3 its normal value. This resulted in an elevation of the threshold energy for gamma-ray detection to about 400 MeV. The data at higher energies were too sparse to justify quoting results at more than one energy level. Indeed, no significant intensities were observed from any of the sources examined. Upper limits of the source fluxes above 400 MeV, with 95 percent confidence, were as follows:

Source	Upper Limit (>400 MeV) in in Units of 10^{-6} photons/cm^2-s
Cyg X-1	4.5
Cyg X-2	5.4
Cyg X-3	3.1
Cas A	2.3
Cas B	4.2
Per X-1	4.3

V. Publications and Theses produced under this research grant

A. Publications

1. Absorption of High-Energy Gamma-Rays in the Vicinity of Pulsar NP0532 by B. McBreen, Nature 224 (1969), 893.
2. A Large Area Gas Cerenkov Telescope for High-Energy Gamma-Ray Astronomy, by P. Albats, S. E. Ball, Jr., J. P. Delvaille, K. I. Greisen, D. G. Koch, B. McBreen, G. G. Fazio, D. R. Hearn, and H. F. Helmken, Nucl. Instr. and Meth. 95 (1971), 189-194.
3. Performance of a Gas-Cerenkov Gamma-Ray Telescope, by D. Koch, S. E. Ball, Jr., M. Campbell, J. P. Delvaille, K. Greisen, B. McBreen, G. G. Fazio, D. R. Hearn, and H. F. Helmken, Nucl. Instr. and Meth. 108 (1973), 349-353.
4. Pulsed High-Energy Gamma-Rays from the Crab Nebula, by B. McBreen, S. E. Ball, Jr., M. Campbell, K. Greisen, and D. Koch, Ap. J. 184 (1973), 571-580.
5. Upper Limits of Hard Gamma-Ray Emission from Six X-Ray Sources, by M. Campbell, J. Alexander, S. E. Ball, Jr., K. Greisen, D. Koch, and B. McBreen, Ap. J. 196 (1975), 593-595.
6. Change in the High-Energy Radiation from the Crab, by K. Greisen, S. E. Ball, Jr. M. Campbell, D. Gilman, M. Strickman, B. McBreen, and D. Koch, Ap. J. 197 (1975), 471-479.

7. Further Observations of High-Energy Pulsed Radiation from the Crab, by M. Strickman, S. E. Ball, Jr., M. Campbell, D. Gilman, K. Greisen, D. Koch, and B. McBreen, to be submitted to Ap. J.

Thesis:

M. S.	Paul L. Baker:	Instrumentation for a Low Energy Cosmic Gamma-Ray Ballon Experiment - 1967.
M. S.	Mitchell I. Morgan:	The Calibration of Photomultiplier for Use in a Gas Cerenkov Telescope - 1971
M. S.	Robert E. Reilinger:	Angular and Energy Resoltuion in Gamma-Ray Telescopes - 1972.
Ph.D.	Paul Albats:	Three Experiments in Gamma-Ray Astronomy at Cornell University - 1971.
Ph.D.	Murray F. Campbell:	A High Energy Gamma-Ray Survey of Cygnus and Cassiopeia - 1974.
Ph.D.	David G. Koch:	Development of a Telescope for the Detection of High Energy Cosmic Gamma-Rays - 1971.
Ph.D.	Mark S. Strickman:	Variability of High Energy Radiation from the Crab Pulsar, NP0532 - 1976.

FIGURE CAPTIONS

Fig. 1. Schematic diagram of the telescope.

Fig. 2. Picture of the internal assembly. In the foreground is the veto scintillator, constructed (like the other scintillator) in 12 segments. The person in the background is David G. Koch, one of the principal designers of the telescope. His left hand is near the edge of the mirror, and near one of the phototubes that detect the signal from the scintillator that is hidden by the mirror. The space frame is seen directly and also by reflection in the mirror.

Fig. 3. Pulsed gamma-ray spectrum of NP0532 in the energy range 10-1000 MeV. The dashed line connects the data points of flight 2 with x-ray data in the range 10-300 keV.

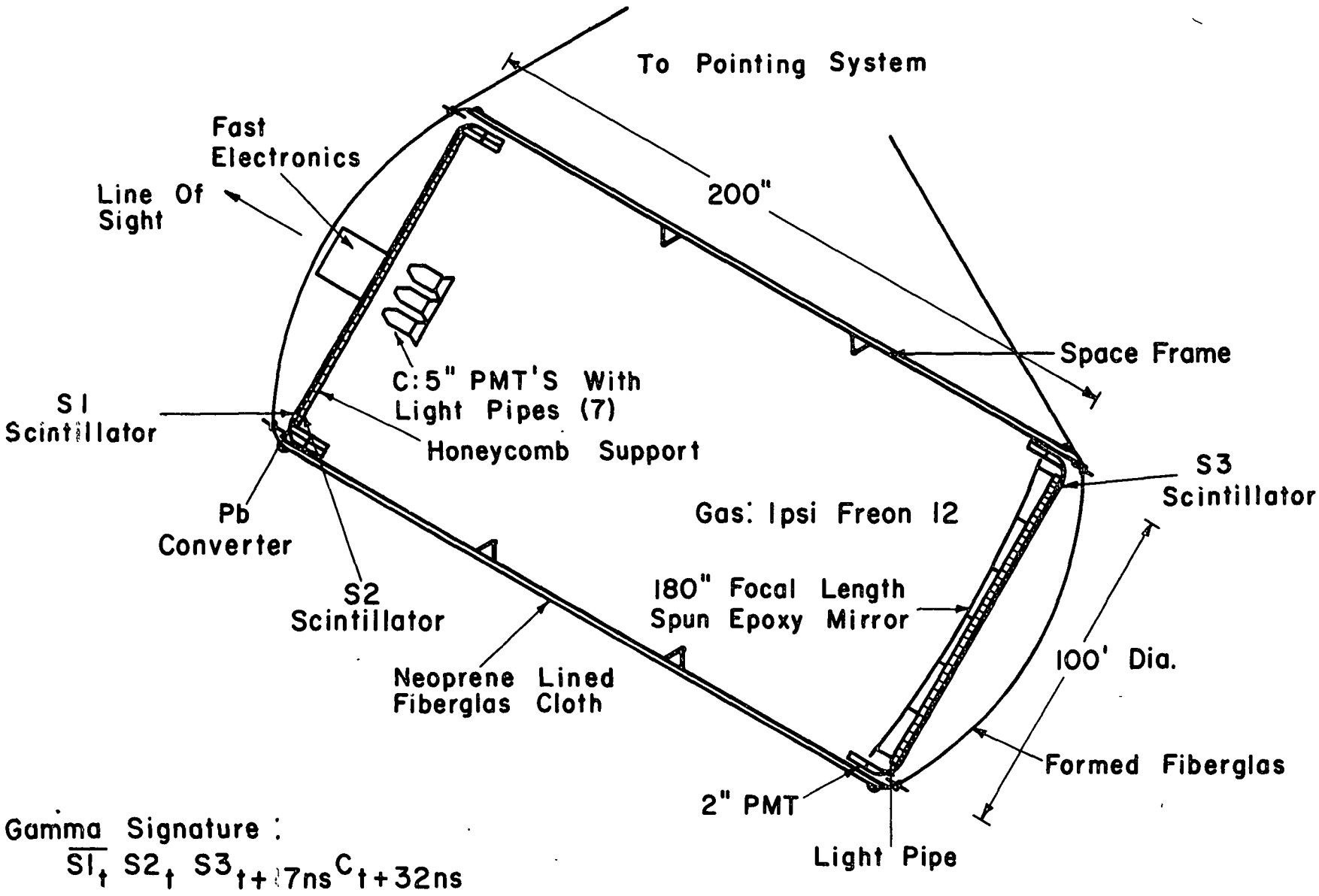

Figure 1. Schematic diagram of the telescope

Figure 2. Picture of the internal assembly

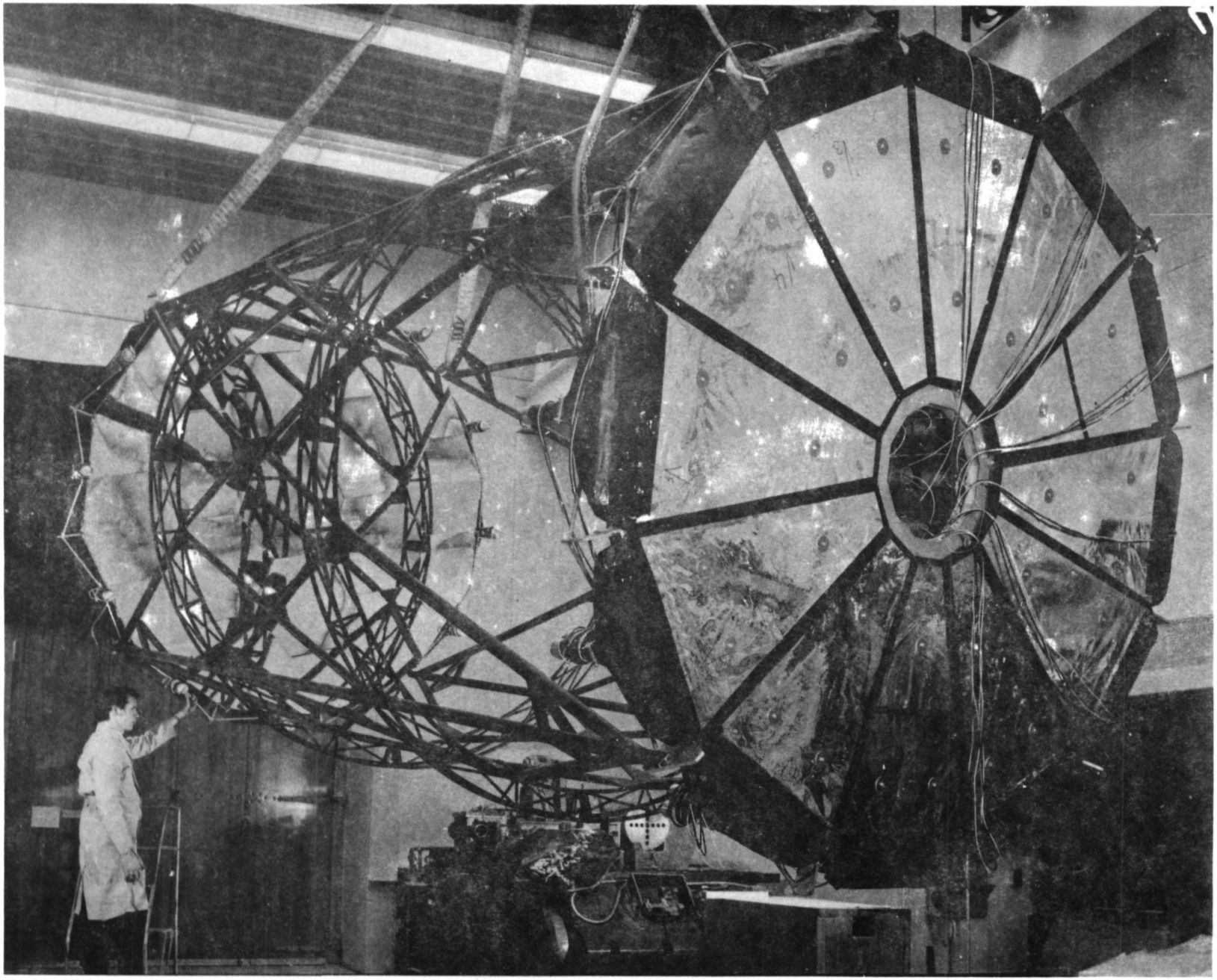

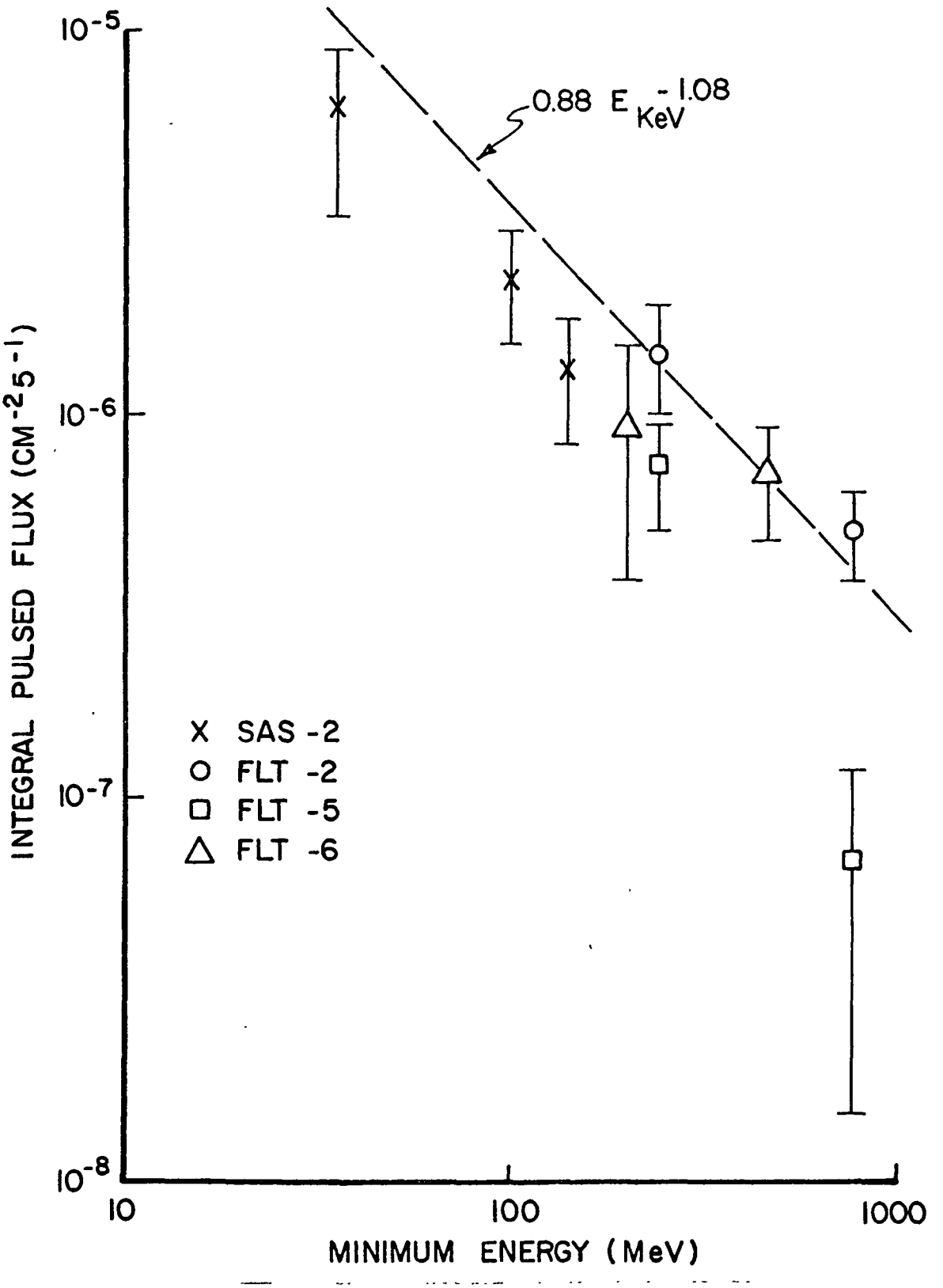

Figure 3: Pulsed Gamma-Ray Spectrum of the Crab Pulsar, NP 0532